



GIS and RS intelligence in delineating the groundwater potential zones in Arid Regions: a case study of southern Aseer, southwestern Saudi Arabia

Mohd Yawar Ali Khan¹ · Mohamed ElKashouty¹ · Ali Mohammad Subyani¹ · Fuqiang Tian² · Waleed Gusti^{1,3}

Received: 30 July 2021 / Accepted: 9 November 2021 / Published online: 22 November 2021
© The Author(s) 2021

Abstract

Proterozoic basement aquifers are the primary source of water supply for the local populations in the Aseer (also spelled “Asir” or “Assir”) province located in the southwest of Saudi Arabia (SA) since high evaporation rates and low rainfall are experienced in the region. Groundwater assets are receiving a lot of attention as a result of the growing need for water due to increased urbanization, population, and agricultural expansion. People have been pushed to seek groundwater from less reliable sources, such as fracture bedrocks. This study is centered on identifying the essential contributing parameters utilizing an integrated multi-criteria analysis and geospatial tools to map groundwater potential zones (GWPZs). The outcome of the GWPZs map was divided into five categories, ranging from very high to negligible potential. The results concluded that 57% of the investigated area (southwestern parts) showed moderate to very high potentials, attributed to Wadi deposits, low topography, good water quality, and presence of porosity and permeability. In contrast, the remaining 43% (northeastern and southeastern parts) showed negligible aquifer potential zones. The computed GWPZs were validated using dug well sites in moderate to very high aquifer potentials. Total dissolved solids (TDS) and nitrate (NO_3^{2-}) concentrations were highest and lowest in aquifers, mainly in negligible and moderate to very high potential zones, respectively. The results were promising and highlighted that such integrated analysis is decisive and can be implemented in any region facing similar groundwater expectations and management.

Keywords GWPZs · GIS · RS · Aquifers · TDS · Aseer · Saudi Arabia

Introduction

Groundwater is one of the most valuable and finite reserves stored underground and is invariably precious to aquatic, human, and terrestrial ecosystems (Fitts 2002; Khan and Wen 2021). Geomorphic features, slope of the area, lithology, geologic structures (joints/lineaments/faults), and drainage networks are some of the most important factors responsible for the occurrence and distribution of groundwater resources (Teeuw 1995; Gyeltshen et al. 2020). Over the past decades, the world’s semi-arid and arid regions have dramatically led to an increased demand for water which has constantly placed a tremendous burden on the reserved freshwater resources. For developing countries such as Saudi Arabia (SA), groundwater has always been considered an important water source for domestic, industrial, and agricultural use (Kumar et al. 2014, 2017, 2020). Groundwater supplies are gradually decreasing and not being fully restored as a result of fast population increase, industrialization,

✉ Mohamed ElKashouty
mohamedkashouty@yahoo.com; melkashouty@kau.edu.sa

Mohd Yawar Ali Khan
makhan7@kau.edu.sa

Ali Mohammad Subyani
asubyani@kau.edu.sa

Fuqiang Tian
tianfq@tsinghua.edu.cn

Waleed Gusti
wagusti@kau.edu.sa

¹ Department of Hydrogeology, Faculty of Earth Sciences, King Abdulaziz University, Jeddah 21589, Saudi Arabia

² Department of Hydraulic Engineering, School of Civil Engineering, Tsinghua University, Beijing 100084, China

³ Department of Environmental Sciences, Faculty of Meteorology, Environment and Arid Land Agriculture, King Abdulaziz University, Jeddah 21589, Saudi Arabia

and overexploitation of aquifer systems (Rodell et al. 2009; Kumar et al. 2021; Mishra et al. 2021). Monitoring hydrogeological research with systematic data integration allows speedy and cost-effective delineation of potential groundwater areas (Barik et al. 2017). Geophysical and hydrogeological surveys, outcrop mapping, logging, etc., are the most common approaches used to detect GWPZs and mapping, but these methods are often time-consuming and expensive (Israil et al. 2006; Jha et al. 2010). In contrast, remote sensing (RS) and Geographic information system (GIS) technologies provide exceptional platforms that can be used to assess natural resources; due to their low-cost efficiency and ability to establish complex spatial data analysis and Spatio-temporal data of a vast space over a short period (Wieland and Pittore 2017; Souissi et al. 2018).

To demarcate GWPZs and mapping, several researchers in the last two decades, have used different multivariate and bivariate statistical techniques (Table 1) with different precision viz. weight-of-evidence model (Tahmassebpour et al. 2016; Corsini et al. 2009), probabilistic frequency ratio model (Manap et al. 2014; Moghaddam et al. 2015), fuzzy-gamma (Antonakos et al. 2014), Shannon's entropy (Naghbi and Pourghasemi 2015), multi-criteria decision making analysis (Singh et al. 2018; Sandoval and Tiburan 2019; Brito et al. 2020), random forest machine learning techniques (Golkarian et al. 2018; Prasad et al. 2020), artificial neural network studies (Lee et al. 2012; Li et al. 2019), machine learning ensembles (Kamali Maskooni et al. 2020), evidential belief function (Nampak et al. 2014), and logistic regression methods (Chen et al. 2018).

Among the various techniques, GIS and RS act as influential, fast in producing results, and cost-effective (Oh et al. 2011) compared to common methods of hydrogeological surveys and have enormous implications in groundwater exploration in water-scanty terranes of hard rock (Jha et al. 2010). Groundwater can only be predicted indirectly by using RS data as it does not occur on the surface. Numerous researches have already been used GIS and RS methods to map and delineate GWPZs (Arulbalaji et al. 2019; Fildes et al. 2020; Mukherjee and Singh 2020). Sener et al. (2005) stated that RS techniques could efficiently recognize features of the earth's surface (for example, geology and lineaments) and can also be utilized to observe groundwater recharge. Mapping of groundwater recharge potential areas by integrating data from RS and GIS techniques was first introduced in India by the National Remote Sensing Agency (Kumar 1987). In recent decades, many researchers have shown great attention in this field and have used GIS and RS methods for groundwater exploration (Teevw 1999; Jha et al. 2010; Deepa et al. 2016; Chen et al. 2018; Kamruzaman et al. 2020). RS data is used for qualitative groundwater resources estimation by analyzing and extracting surface morphology, geological structures, and hydrological

markings. In addition, it provides an improved overview and organized analysis of many geomorphic units, linear features, and topography that control groundwater environments (Singhal and Gupta 1999).

The GIS was applied to utilize, manage, and distinguish RS products, explore locations, merge potential factors of groundwater recharge, and produce suitable weight relations (Sener et al. 2005). Previously, the topography, lithology, and geological features of the Salt River (Western Australia) were derived using satellite information and aerial photos (Salama 1997). Similarly, the groundwater recharge zone and mechanism of groundwater flow can also be determined by these techniques. Krishnamurthy and Venkatesa (1996) utilized GIS and RS approaches to prepare and analyze several thematic maps. They utilized landforms, surface water bodies, lithology, lineaments, drainage density, land use maps, and slope classes to identify the GWPZs in India. Sreedhar et al. (2009) uses hydro-geomorphological, geological, structural, slope, drainage, and land use/land cover to demarcate the aquifer potentiality. Jaiswal et al. (2003) contended that there is a need to manage the GIS and satellite data to concur with the on-site geology, mainly in characteristic terrain hard rock (present study area), where groundwater occurrence is limited and complex (Algaydi et al. 2019).

According to World Bank (2005), the condition of freshwater in SA will deteriorate and be of concern by 2025 if appropriate plans are not made. The two main environmental factors that are primarily responsible for the country's meager surface water resources are high aridity and low precipitation; this poses the need to improve knowledge and mapping of the existing freshwater resources in the country. In SA, the aquifer comprises jointed, fractured, and faulted hard rocks with alluvium deposits. Located in the southwest of the SA, Aseer province represents one of the promising regions for agricultural expansion and tourism (Fig. 1). Groundwater is the only water resource for domestic, agricultural, and industrial use in this region. The basin's terrain elevation is large and steep (reaches 3000 m), implying that the maximum precipitation turns into runoff and quickly flows directly to the ocean. The freshwater crisis due to climate change is also one of the major problems that Aseer is currently facing. The continuous increase in population growth, agriculture, industry, and pollution requires more water consumption, increasing the water problem. However, the scientific board is trying to manage water usage to overcome this problem. In Aseer, the detection and management of aquifers are of great concern due to the need for water supply.

Based on the issues mentioned above, this study aims to identify potential areas for aquifer recharge by integrating RS and GIS techniques in Aseer province. The current research deals with the impact of geological, hydrological,

Table 1 Recent groundwater studies using remotely sensed data and different statistical methods

| Locality | Groundwater influencing parameters used | Number of input parameters | Methods used | Validation | Literature |
|---|--|----------------------------|---|--|-------------------------------|
| Bacao and Northern Bonfim complexes, Brazil | HAND, Slope, Lithology, Morphological lineaments density, Radiometric lineaments density, and Magnetometric lineaments density | 6 | Analytical Hierarchy Process (AHP) | Specific capacity data from deep wells | Brito et al. (2020) |
| Arabian Peninsula in the northern UAE | Elevation, Slope, Precipitation, Geology, Geomorphology, Drainage Stream density, Fracture distance, and Lineament density | 8 | Weighted overlay and random Forest analysis | Well yield data | Al-Ruzouq et al. (2019) |
| Southern Western Ghats, India | Geology, Geomorphology, LULC, Lineament density, Soil, Drainage density, Slope, Rainfall, TWI, Roughness, TPI, and Curvature | 12 | AHP and GIS | Well yield data | Arulbalaji et al. (2019) |
| Al-Ahsa region, Saudi Arabia | Geology, Soil, Slope, Lineament density, Drainage density, Lithology, Rainfall, and LULC | 8 | Geospatial decision making | Water well | Mumtaz et al. (2019) |
| Cold desert, India | Geology, LULC, Hydrogeomorphology, Slope, Lineament density, Drainage density, and Groundwater level | 8 | Frequency ratio model | Spring wells | Balamurugan et al. (2017) |
| Loni and Morahi watersheds, Uttar Pradesh, India | Geology, Geomorphology, LULC, Drainage density, Water table fluctuation, Slope, Soil, and Rainfall | 8 | Multi-criteria decision analysis | Well yield data | Agarwal and Garg (2016) |
| Ilam Plain, Iran | Lithology, Land use, Distance from the river, Soil texture, Drainage density, Altitude, Curvature, TWI, Slope, Lineament density, and Rainfall | 11 | Weights-of-evidence and evidential belief function models | Groundwater wells | Tahmassebiipoor et al. (2016) |
| Beheshtabad Watershed, Chaharmahal-e-Bakhtiari Province, Iran | Lithology, Land use, Fault density, River density, Distance from faults, Distance from rivers, Topographic wetness index, Stream power index, Slope length, Profile curvature, Plan curvature, Altitude, Slope aspect, and Slope angle | 14 | Bivariate and Multivariate Statistical methods | Spring wells | Naghbi and Pourghasemi (2015) |

Table 1 (continued)

| Locality | Groundwater influencing parameters used | Number of input parameters | Methods used | Validation | Literature |
|--|--|----------------------------|---|-----------------------------------|-------------------------|
| Southern part of Selangor State and the northern part of Negeri Sembilan, Malaysia | DEM, Slope, Lineament, Lineament density, Lithology, Soil, Curvature, River density, and Land use | 8 | Frequency ratio method | Well Yield Data | Manap et al. (2014) |
| Kachchh District, Gujarat, India | Lithology, Geomorphology, Lineament density, Drainage density, Soil, Slope, Rainfall, LULC, and DEM | 9 | Weighted overlay analysis | Well yield data | Mukherjee et al. (2012) |
| Sinai Peninsula, Egypt | Lithology, Net groundwater from recharge, Rainfall, Lineament density, Depth to water table, Groundwater quality, Drainage density, and Terrain slope | 8 | Remote sensing and GIS-based modeling | Borehole yield data | Elewa and Qaddah (2011) |
| Udaipur district, Rajasthan, India | Geology, Geomorphology, Soil, Post-monsoon groundwater, Net recharge, Slope, and Proximity to surface water bodies | 7 | Remote sensing, GIS, and MCDM techniques | Well discharge data | Machiwal et al. (2011) |
| Pohang City, Korea | Hydrogeological units, Soil texture, Lineament frequency, Lineament length, Cumulative watershed area, River density, TWI, Curvature, Mean ground slope within the watershed area, Ground slope, Mean ground elevation within the watershed area, Ground elevation | 15 | Probabilistic model | Specific capacity | Oh et al. (2011) |
| Sultan Mountains, Konya, Turkey | Geology, Aspect, Flat, Curvature, Drainage density, Fault density, Distance to drainage, Elevation, Profile curvature, Slope, Wetness index, LULC, and Relative permeability | 0 | Frequency ratio, weights-of-evidence, and logistic regression methods | Spring wells | Ozdemir (2011) |
| Pavagadh, Gujarat, India | Lineament density, DEM and Slope, Drainage density, and LULC | 4 | Remote sensing and GIS | Pumping station data | Pumping station data |
| West Medinipur district, West Bengal, India | Geology, Geomorphology, Recharge, Drainage density, Soil, Slope, and Distance from the surface water body | 7 | Weight assignment and GIS-based modeling | Average groundwater level decline | Chowdhury et al. (2010) |

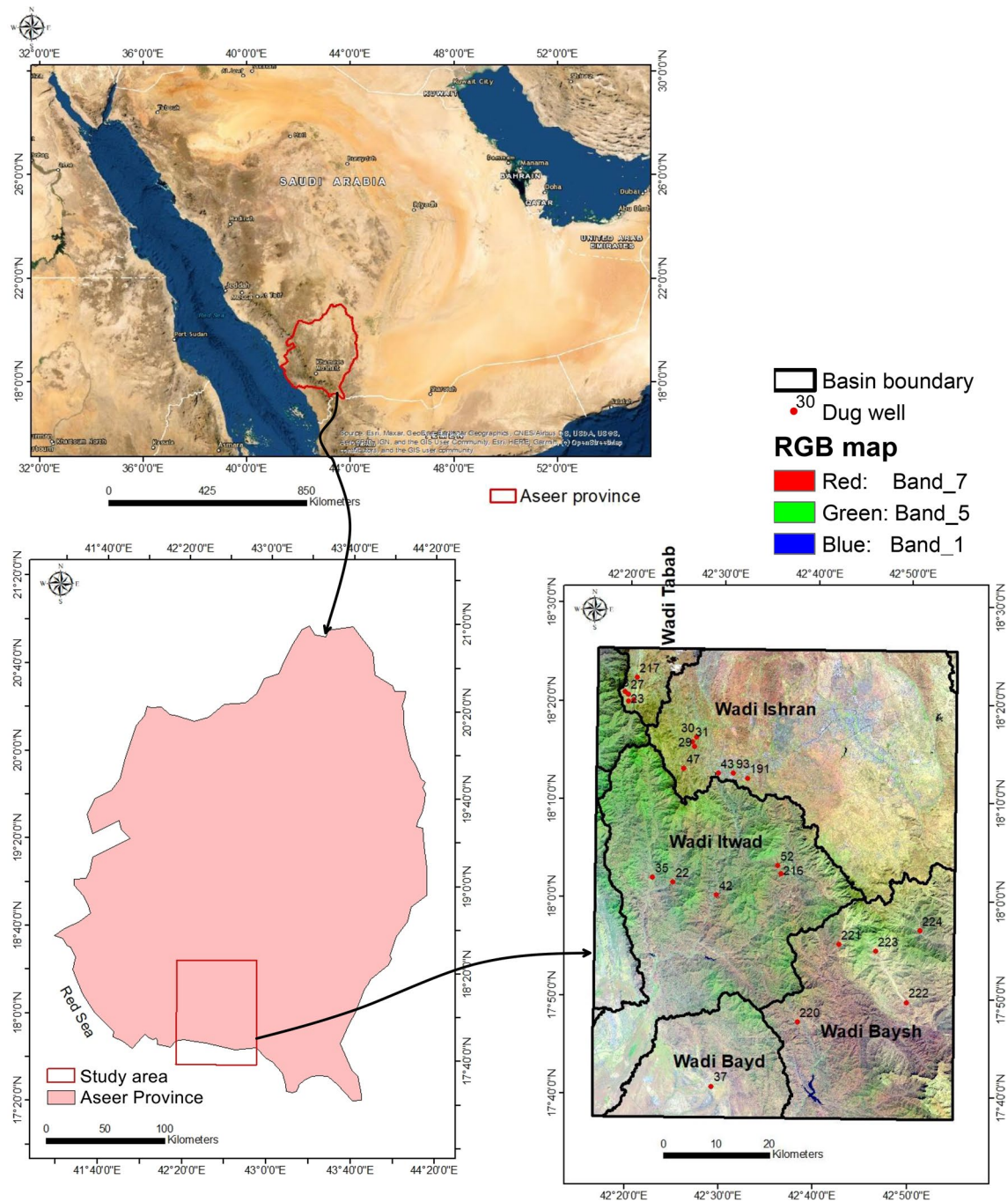


Fig. 1 Location map of the study area

and hydrogeological layers on the aquifer and is subsequently assessed to build up the GWPZs map. These layers were created utilizing multiple geospatial methodologies to assess aquifer potentiality in thematic maps such as lithology, stream networks, lineament, digital elevation

model (DEM), slope, rainfall, and normalized difference vegetation index (NDVI). The study's outcomes are promising because it allows sustainable use of aquifer resources, increases income/capita, and improves the good management of groundwater sources.

Study area

The study area is located in the southern portion of the Aseer province and mainly comprises the part of Abha and Khamis Mushait city. It covers 5969 km square (km²), which is 7.5% of the total area of Aseer province and is located between 17°40'0" N to 18°30'0" N, and 42°20'0" E to 42°50'0" E in the southwestern portion of the SA (Fig. 1).

The area's elevation ranges between 30 and 3000 m above mean sea level (MSL), with an average of 1530 m. The climate is warm and temperate (Fig. 2). With an average temperature of 19 °C, the warmest month of the year is June (average temperature of 23.8 °C), and January is the coldest month of the year (average temperature of 13.6 °C) (<https://worldweather.wmo.int>).

It has been observed that rainfall occurs more in summers than winters, caused by wet oceanic winds carried by the southwestern monsoon (Vincent 2008). The driest months are from October–December, with a mean rainfall of 13 mm and reach its peak in the months from March–August, with an average rainfall of 24 mm. The mild climate of the study area makes it a popular tourist destination for Saudi people. Hence the quality of groundwater is impacted by the projects associated with its rapid development and tourism.

Geology

The study area is covered by rock units ranging from Proterozoic to Cenozoic age (see Fig. 8a). It exists in meta-volcanic and meta-sediments, mainly represented by Baish and the Abha groups and the Sabya Formation (Blank et al.

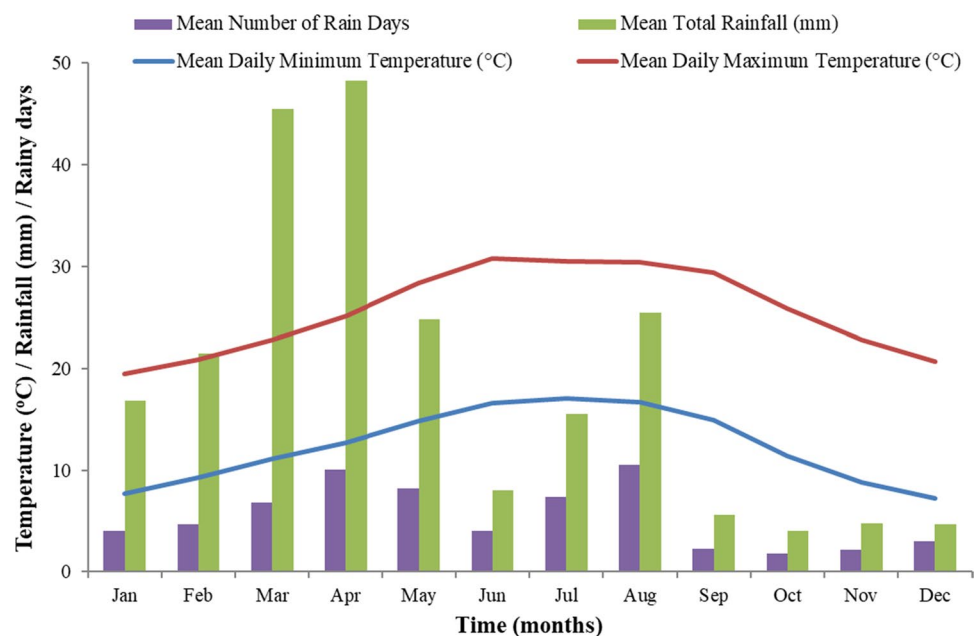
1985). The lithology of the study area ranges from diorite, basalt, and gabbro. The area has been exposed to various tectonic activities from the Cambrian to the Quaternary period, accentuated with the Red sea opening (Oligo– Miocene). Faults and joints are the notable structural features of the area with elongated grabens, and horsts are formed due to the NE-SW faults (Mogren et al. 2011). Following the main fracture system, that is, running perpendicular to the Red sea's direction, the main Wadis in the area are trending from west to east (Hussain and Ibrahim 1997).

Hydrogeology

Based on field investigation, most of the aquifer in the investigated area comprises fractured and jointed hard rocks and is subsequently recharged by precipitation through infiltration. The fractured and jointed hard rocks produce shallow aquifers with varying porosity and permeability, thus changing the aquifer storage coefficient. Deposition of fine sediments in joints, fractures, and faults in the hard rocks reduces the groundwater flow, facilitating runoff leakage and aquifer recharge. The water from these aquifers is pumped through the dug wells by excavating the rocks downward.

The hydrogeochemical study of these aquifers shows excellent water quality for irrigation (TDS mostly does not exceed 2000 mg/L). The concentration of TDS ranges from 228 to 2338 mg/L in Wadi Ishran and Tabab. The high value of TDS in these regions is attributed to rock water interactions and the low presence of lineaments. The TDS concentration ranges from 347 to 1216 mg/L in the Baysh, Itwad, and Bayd Basins. The low TDS value in these regions is attributed to a larger number of lineaments, leading to

Fig. 2 Average monthly rainfall and average monthly temperature of the study area



higher recharge. The concentration of NO_3^{2-} in most of the groundwater is less than 10 mg/L, except for wells scattered in the Baysh, Itwad, and Tabab Wadis, which exceeded the drinking water guideline 45 mg/L.

Water demand versus supply

SA is located in an arid zone with very limited water resources. Due to low rainfall and high evaporation rates, and SA does not have permanent rivers and lakes (Al-Ibrahim 1991). The country's aquifers store approximately 3,958,000 million cubic meters (MCM) of water (MWE 2012). The average annual recharge rate is 3850 MCM (MWE 2012; World Bank 2005) and affects the management and planning of water resources. The recharge represents a renewable and sustainable annual groundwater yield from the aquifer systems (Ouda 2014).

The demand for water in SA is much higher than the sustainable yield of conventional (groundwater and surface water) and non-conventional (treated wastewater and desalinated water) water resources. This gap is

mainly related to groundwater scarcity. Water demand has increased over time, especially in the industrial and agricultural sectors (Fig. 3a). SA population growth is likely to double by 2030 (Fig. 3b), and hence the water supply will likely increase from 6400 MCM/y in 2010 to 10,158 MCM/y in 2030 (Fig. 3c). This increase in the water supply is associated with expanding non-conventional resources and roughly from surface waters (Ouda 2014). Over time the demand for the water has increased dramatically; however, the groundwater yields have remained constant (Fig. 3c).

Figure 3d shows that in 2025 and 2030, the projected gap between water demand and supply will decrease with the decline in agricultural activity. The decline in income/capita will have an impact on policy making and subsequently on people. This study aims to identify alternative water resources to reduce the gap and increase investment in the agricultural sector. To minimize the gaps in supply and demand in future, intensive measures are needed to manage water demand in all sectors, especially for the largest consumers of water (agriculture).

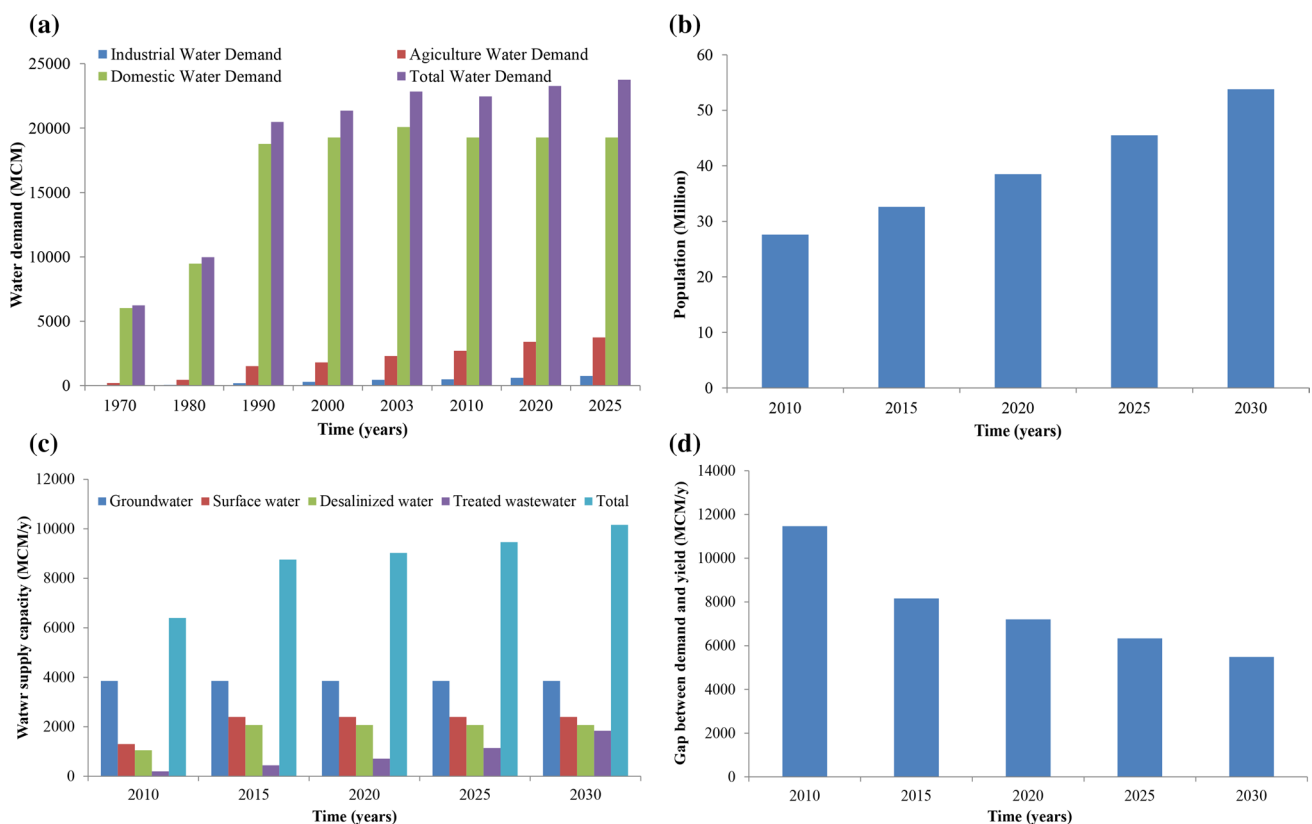


Fig. 3 Current and predicted **a** water demand in different sectors **b** population **c** water supply capacity and **d** gap between water demand and supply (Ouda, 2014)

Methodology

Objectives

The main objectives of the present study are the assessment and evaluation of the GWPZs based on thematic maps such as stream network, lineaments, geology, slope, rainfall, DEM, and NDVI. These thematic maps were prepared and integrated using RS and GIS techniques to produce GWPZs. RS and GIS techniques are effective in the management and planning of drainage basins and aquifers. The continuous updating of these techniques gives us spatial data integration for aquifer management (Rao and Jugran 2003).

Data sets

Two images of the Shuttle Radar Topography Mission (SRTM) -DEM were downloaded from the United States Geological Survey (USGS) website (<https://earthexplorer.usgs.gov/>). These images were mosaicked to demonstrate the research area being studied. Two Landsat 8 surface reflectance (L8SR)—Enhanced Thematic Mapper Plus (ETM+) images (path 167/row 047; SCENE ID: LC81670472018326LGN00 and path 167/row 048; SCENE ID: LC81670482018326LGN00) with 30 m resolution were downloaded from USGS website (<https://earthexplorer.usgs.gov/>). The L8SR images contain 11 bands and a low cloud cover (0.02). These images were corrected for wavelengths, quick atmospheric pressure, UTM projection WSG84, and contrast stretching. NDVI was determined from the L8SR images to display green vegetation (hydrogeology). The digital number (DN) of L8SR images were transformed to reflectance values according to the following equation:

Band specific reflectance multiplication band

$$* \text{ DN values} + \text{ reflectance additive band}$$

It is corrected for sun angle by meta data included in the satellite images information as.

$$\text{Reflectance} / \sin (\text{sun elevation}) \quad (1)$$

The NDVI was calculated by the following formula.

$$\text{NDVI} = (\text{NIR} - \text{Red}) / (\text{NIR} + \text{Red}) \quad (2)$$

where NIR = near-infrared band and Red = red band.

The geological map was scanned and geo-referenced using L8SR images, and distinct rock units were digitized. The digitized geology is a valuable source of data for the supervised image classification accuracy assessment (Maximum Likelihood) (ML) classifier. Land cover classes were extracted from L8SR images to prepare a base map for the area studied. The ENVI v 5.1 software was used for digital

image processing and pre-processing of the data was done to build a mosaic of two images. ArcGIS 10.3 software packages have been used to obtain flow network, geology, slope, DEM, and NDVI. Lineaments were extracted using ENVI v 5.1 software and subsequently went through automatic extraction lineaments (PCI Line software), handling extraction lineaments (ArcGIS 10.3 software), and finally for trend analysis (RockWork v 16 software). The principal component image (PCI) carries the most information and is suitable for lineaments extraction purposes (PCI Geomatica). Using ArcGIS 10.3 with L8SR images and other source data, thematic maps were prepared for flow network, lines, geology, slope, rainfall, DEM, and NDVI. Attribute values were assigned for each theme according to classification.

The UTM-WGS 84, Zone 38 North (projection coordinate system) were used to project all layers. With a common weight scale of 1–5, thematic maps were converted and reclassified to raster images. Based on the potentiality of the aquifer from very high to very low potential, the classes were allocated for the theme. Weighted overlay analysis was used to integrate the output raster maps. The overlay analysis (prospect map) was classified into five classes ranging from very low to very high potentiality. Figure 4 illustrates the methodology used for the current study. Weighted overlay analysis and interpolation method are the two inverse distance weighted (IDW) procedures of the spatial analyst tools in ArcGIS software used to construct thematic layers to extract the aquifer potentiality.

Results and discussion

The thematic maps representing stream network, lineaments, geology, slope, rainfall, DEM, and NDVI were supervised to produce the GWPZs map. The most relevant geological, hydrological, and hydrogeochemical characteristics that contribute to the aquifer's recharge are chosen using this method. The stream network represents aquifer storage and surface runoff, while the lineaments represent secondary rainwater leakage conduits. The geological formation indicates the exposed sediments' percolation capacity. The slope influences the runoff remains running on the earth's surface. The NDVI classifies the landform based on vegetation intensity, which in turn reflects the more aquifers to be used. The input layers were arranged numerically, as shown in Table 2. The arranged layers were determined based on contribution to the groundwater recharge. Each layer was divided into classes, reflecting the aquifer potentiality control (Table 2). All the weighted layers were integrated through GIS and produced groundwater potential map (e.g., Eastman et al. 1995).

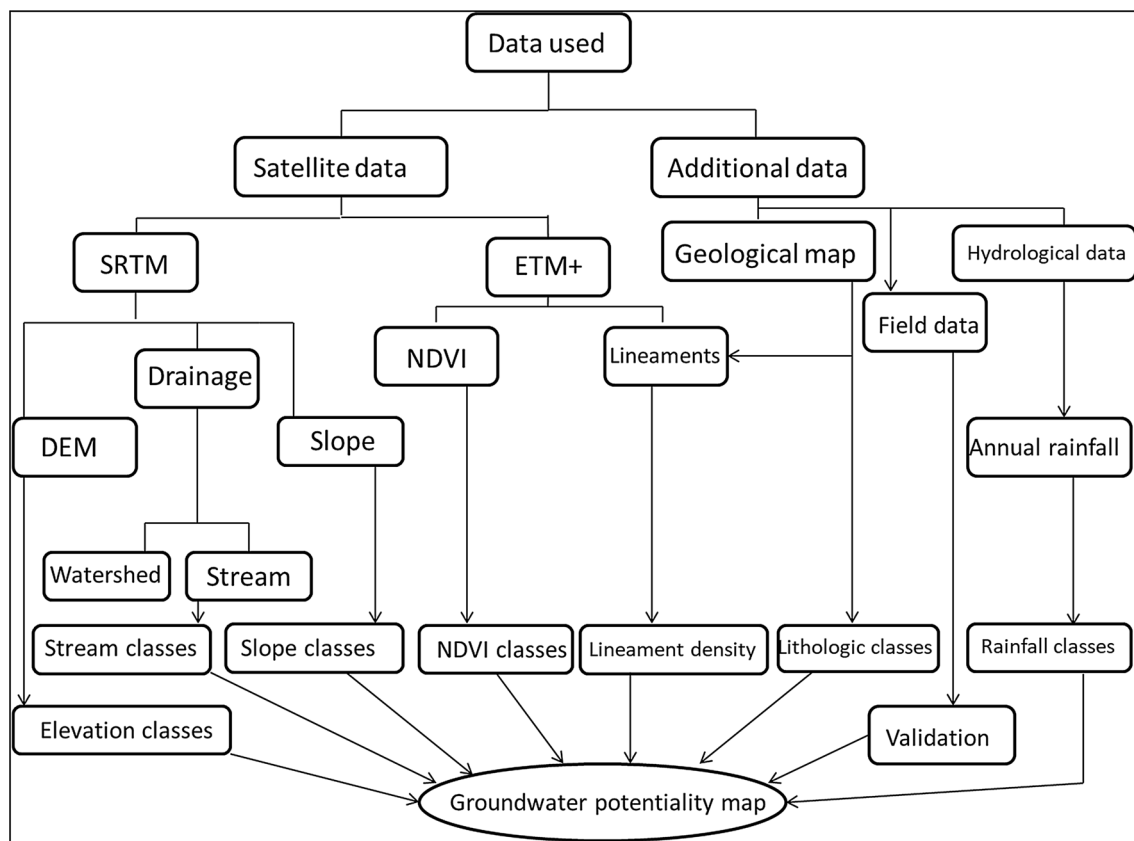


Fig. 4 Flow chart summarizing the approaches followed

Topography layer

The land elevation estimates the runoff flow direction and defines the aquifer determination. The DEM clarifies the elevation ranging from 0.0 to 2994 m (Fig. 5a).

The land elevation ranges from 30–525 m in the southwest to 1719–2994 m in the northeast (Fig. 5a). The fluctuation in elevation increases the slope differences, impacting surface water flow toward the lowest elevation areas (southwest, Fig. 5a, b). The DEM map was subdivided into five classes of 30–525 m, 525.1–1080 m, 1080.1–1719 m, 1719.1–2280 m, and 2280.1–2994 m corresponding to very high, high, moderate, low, and very low aquifer potentiality, respectively (Table 2). Based on elevation contribution to aquifer recharge, about 37% of the investigated area was categorized by very low to low aquifer potential and 52% by high to very high potential (Fig. 5b).

Slope layer

The topographic slope influenced the aquifer recharge, surface runoff, and leakage. The leakage evaluates the aquifer potentiality zones (Sreedhar et al. 2009). A gentle slope is characterized by a low surface runoff velocity, is suitable for water leakage, and increases aquifer recharge. On the other hand, rapid runoff is detested in steep slopes, and thus there is less or no chance of aquifer recharge and infiltration. The land’s slope was inversely proportional to runoff leakage. The slope ranged from 0 to 79 degrees (Fig. 6a), estimated by the DEM. Das and Pal (2019) stated that the undulating terrain impact slope values. The slope map is classified into five classes of very low potentiality, low potentiality, moderate, high potentiality, and very high potentiality corresponding to the slope of 79–35.1, 35–25.6, 25.5–16.3, 16.3–7.7, and 7.7–0, respectively (Fig. 6b).

Table 2 Thematic map weights and capability values

| Thematic layer | Map rank/Total | Map weight (wt) | Class ranges | Degree | Rank | Capability value (CV) | |
|---|----------------|-----------------|-------------------------------------|-----------|------|-----------------------|--|
| 1- Stream network (Drainage density) | 3/18 | 0.17 | 1–58 | Very low | 1 | 0.07 | |
| | | | 58–120 | Low | 2 | 0.13 | |
| | | | 120–189 | Moderate | 3 | 0.20 | |
| | | | 189–285 | High | 4 | 0.27 | |
| | | | 285–713 | Very high | 5 | 0.33 | |
| 2- Lineaments (as density) | 3/18 | 0.17 | 0–0.05 | Very low | 1 | 0.07 | |
| | | | 0.06–0.14 | Low | 2 | 0.13 | |
| | | | 0.15–0.28 | Moderate | 3 | 0.20 | |
| 3- Geology (formation) | 2/18 | 0.11 | 0.29–0.47 | High | 4 | 0.27 | |
| | | | 0.48–0.80 | Very high | 5 | 0.33 | |
| | | | Greenstone and schistose greenstone | | | | |
| | | | Andesite diabase | High | 3 | 0.5 | |
| | | | Amphibolite and schist | | | | |
| 4- Slope (degrees) | 2/18 | 0.11 | Marble, quartzite, and syenite | Moderate | 2 | 0.33 | |
| | | | Granite and granodiosite | Low | 1 | 0.17 | |
| | | | 0–7.7 | Very high | 5 | 0.33 | |
| | | | 7.7–16.3 | High | 4 | 0.27 | |
| | | | 16.3–25.5 | Moderate | 3 | 0.20 | |
| 5- NDVI | 1/18 | 0.06 | 25.6–35 | Low | 2 | 0.13 | |
| | | | 35.1–79 | Very low | 1 | 0.07 | |
| | | | (–0.5)–0.1 | Very low | 1 | 0.07 | |
| | | | 0.11–0.16 | Low | 2 | 0.13 | |
| | | | 0.17–0.124 | Moderate | 3 | 0.20 | |
| 6- Annual rainfall (mm) | 4/18 | 0.22 | 0.25–0.35 | High | 4 | 0.27 | |
| | | | 0.36–0.84 | Very high | 5 | 0.33 | |
| | | | 181.8–191.6 | Very low | 1 | 0.07 | |
| | | | 191.7–200.4 | Low | 2 | 0.13 | |
| | | | 200.5–208.5 | Moderate | 3 | 0.20 | |
| 7- DEM (m) | 3/18 | 0.17 | 208.6–217.1 | High | 4 | 0.27 | |
| | | | 217.2–230.3 | Very high | 5 | 0.33 | |
| | | | 30–525 | Very high | 5 | 0.33 | |
| | | | 525.1–1080 | High | 4 | 0.27 | |
| | | | 1080.1–1719 | Moderate | 3 | 0.20 | |
| | | | 1719.1–2280 | Low | 2 | 0.13 | |
| | | | 2280.1–2994 | Very low | 1 | 0.07 | |

The ranking interval from low to steep slopes is based on the contribution rate to aquifer recharge (Table 2). From the SRTM map, it was estimated that the highest percentage, i.e., 30% and 32% of the study area was occupied by the very gentle slope (< 8 degrees) and gentle slope (8–16 degrees), respectively (Fig. 6b). These conditions have suitable time that favors the runoff leakage and aquifer recharge.

The dug wells were drilled in the Wadis rather than in higher elevations. On the contrary, higher topography and

hard rocks form steep slopes, which results in a high velocity of surface runoff and consequently low aquifer recharge and high-risk flooding. The zone representing 30% of the study area (< 8-degree slope) is excellent for recharge, as it reduces the runoff, and in turn, helps in the recharge process. In contrast, the zone with a slope of > 16 degrees is less suitable for recharging than a slope of < 8 degrees. Higher weights are assigned to a relatively lower slope due to the higher recharge capacity.

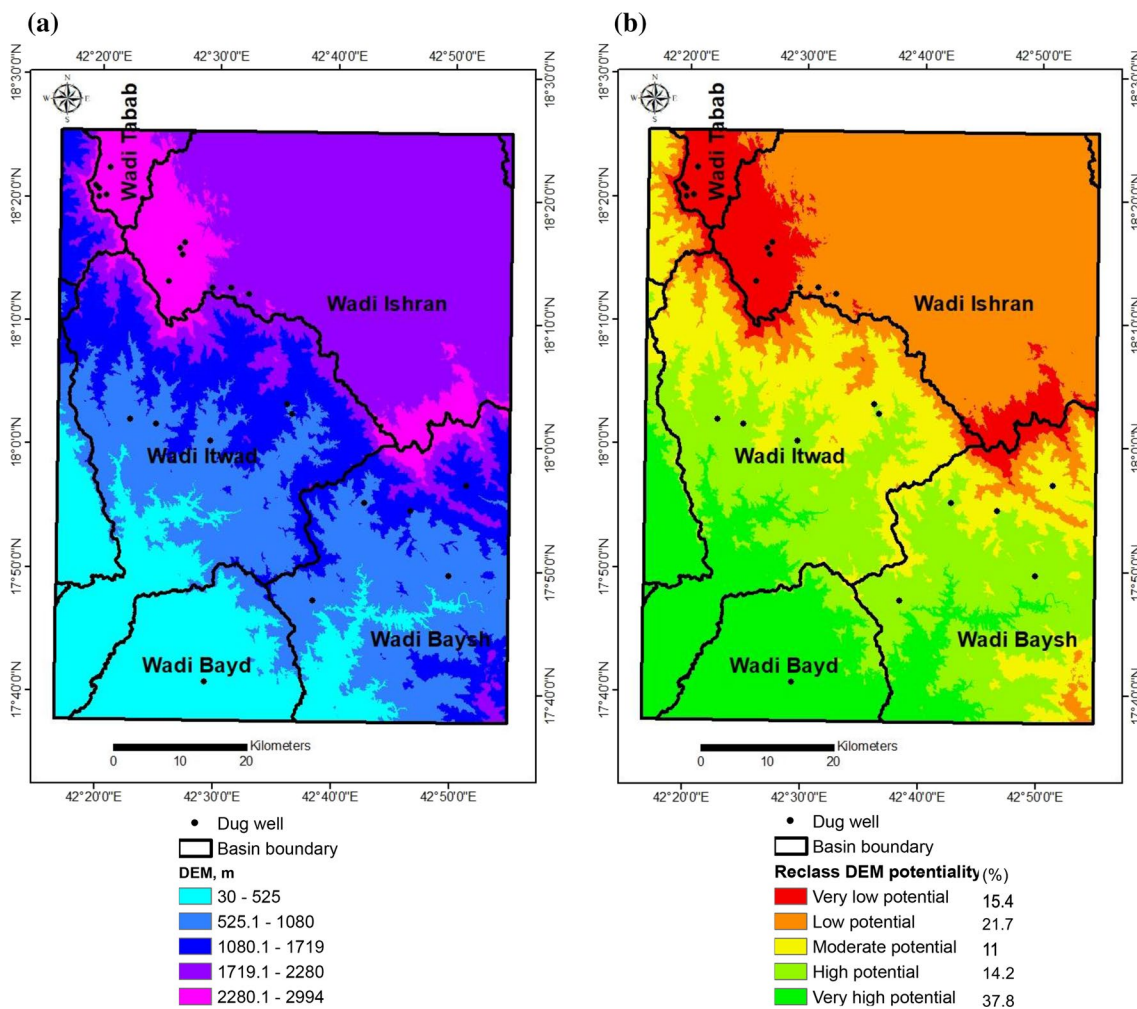


Fig. 5 a Topography and b reclassified topography of the study area

Stream network layer

Morphometric investigation of the drainage basins reflects the hydrogeological conditions. The exposed geology affects the watersheds' texture, configuration, density, and leakage—runoff relationships (Edet et al. 1998). The stream channels and watershed boundaries were extracted from SRTM elevation data. The geology, hard rocks, structural joints, fractures, and faults (lineaments) impact stream channel distribution. The distribution of tributaries in the north and south is dendritic and are exposed mainly as chlorite sericite schist and amphibolite schist in the north, whereas andesite, diabase, amphibolite, and schist in the south (Fig. 8a). The parallel pattern is mainly distributed in the greenstone and schistose greenstone (Figs. 7a, 8a). According to the SRTM map, drainage intensity was assessed and was divided into five classes ranging from very low to very

high potential depending on their influence on water leakage rate (Fig. 7b). Drainage density categories varied from very low to very high (as used in many studies). It was interpreted that the smaller the drainage density, the higher the water layer, and vice versa. Most of the wells drilled in and around the surveyed area were in Wadis with high drainage densities. Therefore, the high drainage density mainly includes production wells, so it has the advantages of being very suitable for aquifer replenishment and reliable permeability. Based on previous concepts, higher classes of drainage density have improved the aquifer recharge. The main channels beds (deposits) are characterized by high drainage density and the location of drilled wells. The very low and low potential regions include 47% and 25.2% of the study area, respectively (Fig. 7b), whereas high to very high potentials represent 11.4% of the study area (Fig. 7b).

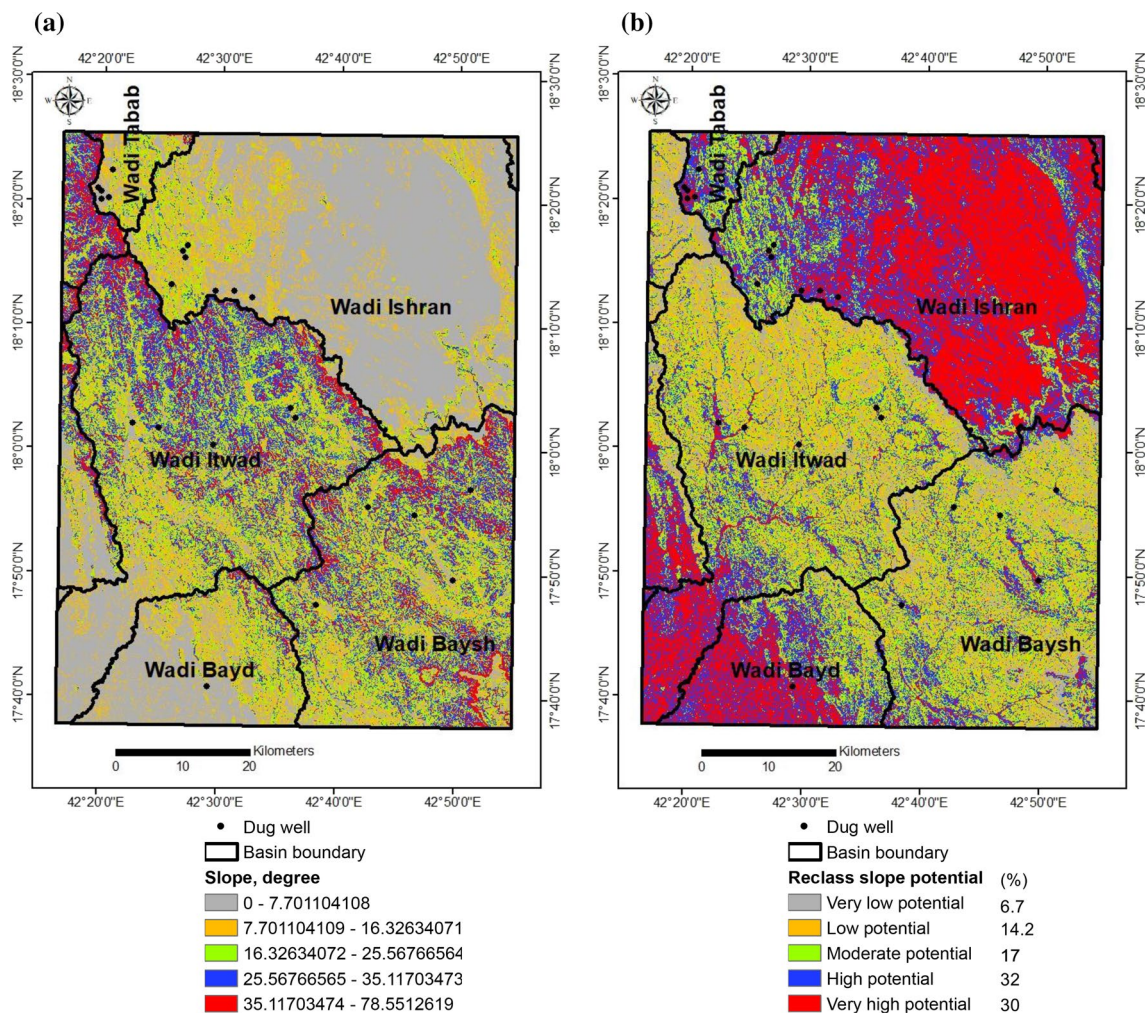


Fig. 6 a Slope and b reclassified slope of the study area

Lithology layer

The aquifer hydrogeological properties influence aquifer recharge and storage. The higher hydraulic conductivity increases the groundwater flow and thus, increases aquifer recharge. The water leakage was affected by the hydrogeological properties of the exposed aquifer. The supervised digital geological map was created from the original georeferenced geological map with an ETM+ satellite image. It is subdivided into seven formations, greenstone, and schistose greenstone; andesite and diabase; amphibolite, schist, and related rocks; granite and syenite; marble, quartzite; chlorite sericite schist, and amphibolite schist; and granite-granodiorite (Fig. 8a). Based on the lithological contribution to aquifer recharge and storage, the study area was subdivided into three classes of low, moderate, and high potential (Fig. 8b). The majority of lineaments in the research area are

found in metamorphic rocks, whereas igneous rocks have a low to medium density of lineaments. The aquifer recharge is more absorbed in shallow depths (near-surface lineaments), which draws investment, rather than deep depths. Higher weights were given to metamorphic rocks for their higher permeability (fractures systems) than those in igneous rocks. The high potential region accounts for 43.4% of the study area (Fig. 8b).

Lineament layer

Lineaments analysis reflects the water leakage through joints, fractures, and faults. The studied areas exposed mainly by hard rocks were characterized by joints, fractures, and faults systems, besides the weathering of the rocks. The lineaments aggregates represent the main recharge for the aquifer and are associated with their

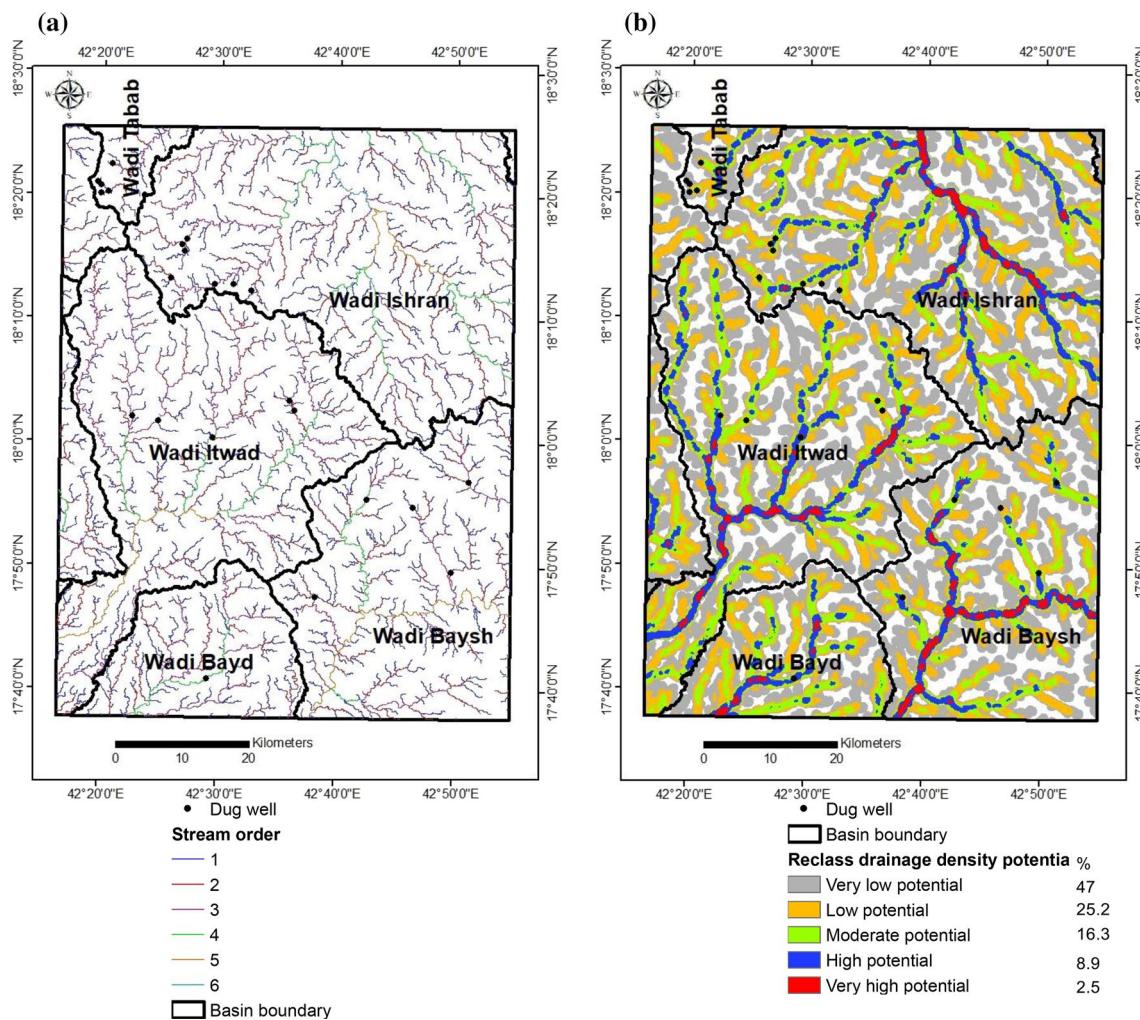


Fig. 7 a Stream network and b reclassified stream network of the study area

higher number, greater lengths, and widths. They serve as conduits and better inter-connections with other fractures (Edet et al. 1998). The lineaments were extracted from the geological map and an ETM + 8 satellite image, that gives us the most important data of the surface and subsurface fractures systems, which impact aquifer storage (Sreedhar et al. 2009; Algaydi et al. 2019). The lineaments density was subdivided into five categories, ranging from very low to very high density (Fig. 9a).

The high to very high lineament density is excellent for aquifer recharge, leakage, and potentiality. The reclassified lineament density map is divided into five classes that vary from very high potential (very high lineaments density) to very low potential (very low lineament density) (Table 2, Fig. 9b). The greenstone and schistose greenstone are highly fractured, while the crystalline rocks (granites and syenites) have low lineament density (Figs. 8a, 9b). Based on lineaments concentration, approximately 86% of the study area had a very low potential for aquifer recharge (Fig. 9b).

Normalized difference vegetation index (NDVI) layer

The vegetation index (VI) reflects green vegetation. The VI estimates the area irrigated by the aquifer and influences the moisture content of the soil.

The VI aims to display and inventory pixels (areas) with green vegetation. The dense vegetation zones reflect intense rainfall and the presence of aquifer potential. NDVI can identify groundwater-rich joints, fractures, and faults systems through vegetation growth. The high to very high VI was found in greenstone and schistose greenstone (Fig. 10a), which offers the highest weights for NDVI and geology. NDVI was classified into five classes based on vegetation concentration and ranged from very low potential (very low VI concentration) to very high potential (very high VI distribution) (Fig. 10b).

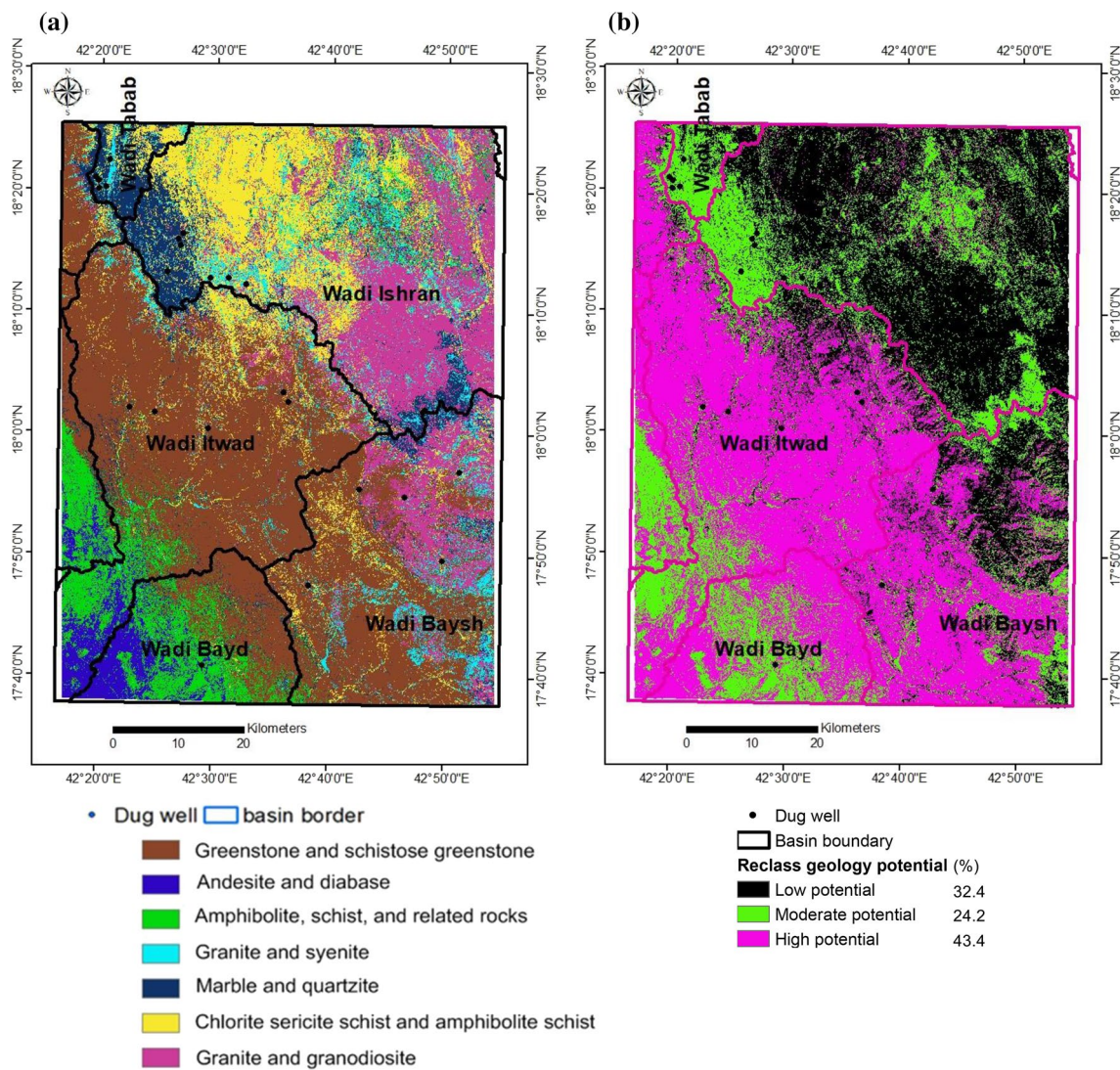


Fig. 8 a Geology and b reclassified geology of the study area

Rainfall layer

Precipitation at Aseer region controls the rate of recharge of the aquifer. The rainfall is highest in the northern part (217–230 mm/year) as compared to northeastern and southern parts (182–192 mm/year) (Fig. 11). The precipitation gradients influence the leakage water and can increase the aquifer potentiality. The precipitation distribution map was determined by spatial analyst tools of GIS (Fig. 11a, b). The proportions of each potential zone are shown in Table 2.

GWPZs map

A map of the aquifer potential has been extracted from various hydrogeological, geological, and hydrological thematic maps and is crucial for agricultural, domestic and industrial applications. Weights were given for each parameter

map, depending on the contribution to groundwater recharge (Table 2). A GIS model combined these thematic maps to forecast the most favorable map of aquifer potential. (Voogd 1983) introduced the multi-criteria evaluation (MCE) technique. The aquifer potential-map was extracted from various geological, hydrogeological, and hydrological thematic maps and is significant in agricultural, domestic, and industrial applications. The weights of each parameter are based on its contribution to groundwater recharge (Table 2). The GIS model was used to predict the most promising map of aquifer potential integrated by these thematic maps. The map rank was transformed into map weight by dividing map rank by summing of parameters ranks (Table 2). The map categories assigned different classes ranging from 1 (lowest

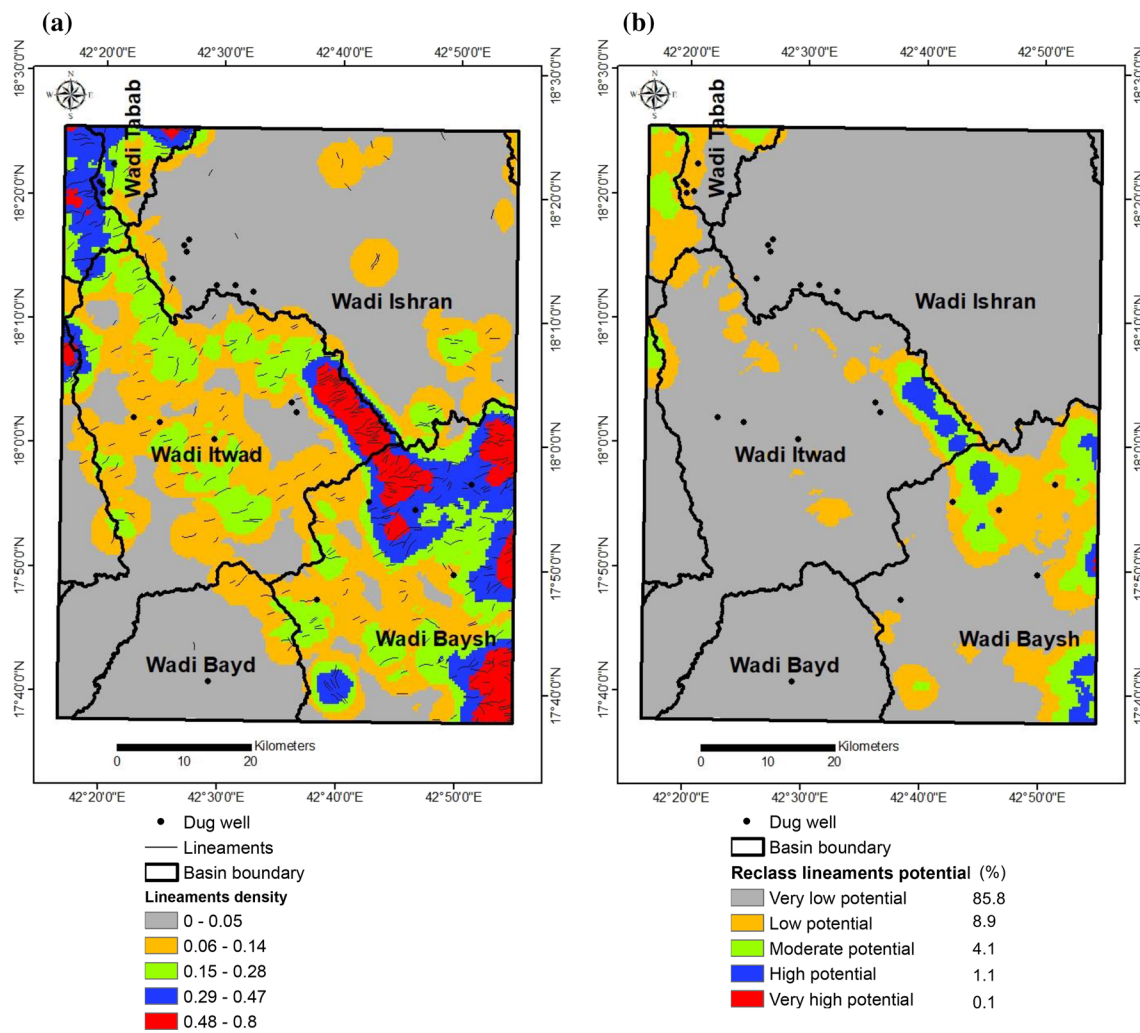


Fig. 9 a Lineaments density and b Reclassified lineament density of the study area

favorable) to 5 (highest favorable, except geology of 1 to 3 (Table 2). The rank of each class was divided by the total clustering values of the layer classes to calculate the capability values (CVs) (Table 2). These CVs are multiplied by the weight of the relevant probability layer in each thematic layer to compute the groundwater probability map (Fig. 12). It is calculated mathematically using the ArcGIS raster calculator analysis as follows:

$$GWP = \sum W_t * CV \tag{3}$$

where GWP is groundwater potential ($GWP = \sum$ Stream network, lineaments, geology, slope, rainfall, DEM, and NDVI), W_t is map weight, and CV is capability value. The aquifer potential map has been classified into five categories,

ranging from very low to very high potentiality (Fig. 12). The Wadi sediments (hard rock debris and alluvium deposits) have good promising areas for groundwater extraction, particularly in the southwestern part (Fig. 12).

The southwestern part comprised high to very high aquifer potential, whereas the northeastern part consisted of low to very low potential (Fig. 12). About 57% of the study area is represented by moderate to very high potential, as shown in Table 2, which is a good indicator for aquifer exploration and exploitation. The low to very low aquifer potential represented 43% of the area (Table 3). The groundwater potential outcomes (Table 3) provide a comprehensive dataset for the groundwater recharge conditions. An aquifer potentiality map provides more information for residents (Bedews) and

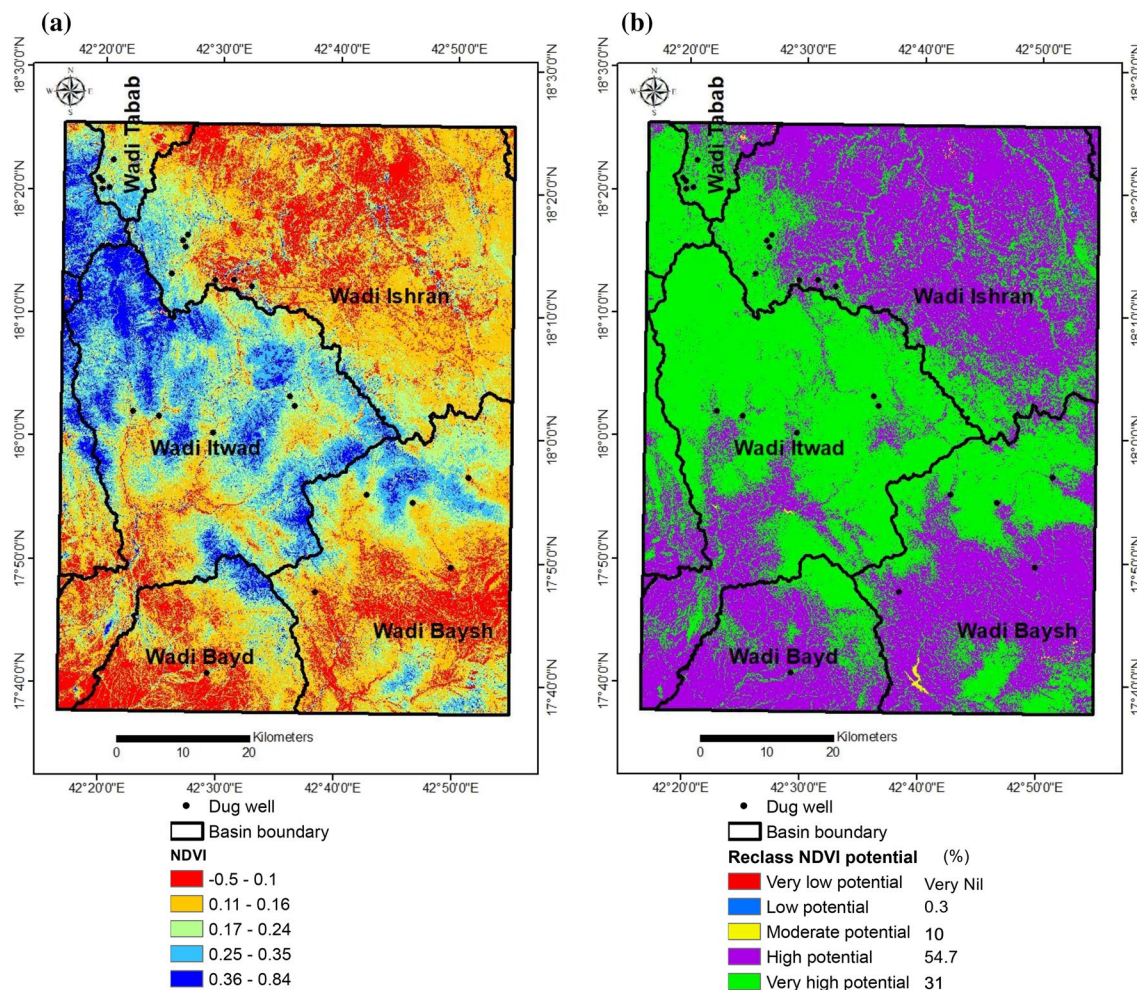


Fig. 10 a NDVI and b Reclassified NDVI of the study area

administration and investors interested in appropriate zones for aquifer pumping and protection against contamination.

Model validation

Dug well sites

Due to the non-availability of abandoned boreholes of groundwater, the outcomes of this study were validated only through available dug wells. The hydrogeochemical characteristics of the groundwater encourage seeking new promising areas for further investment and urbanization. As evident from Fig. 12, most of the dug wells were located in moderate to very high potential zones; the good coincidence reflects excellent aquifer potential model outputs. These results encourage the authorities to invest in the new promising areas with a high to very high aquifer potential (Fig. 12). Due to the lack of well yield data, the validation approach is carried out by matching the resulting GWPZs with the measured TDS and NO_3^{2-} concentration in the dug

well located in the study area, as reported earlier by Schlumberger Water Services (2013) and Mallick et al. (2018). The existence of good water quality well in moderate to very high potentiality zones is considered an excellent output of this study. The basis of this validation implies the existence of successful dug wells (i.e., with high water quality) in the areas depicted as having medium to high potential on the GWPZs map.

Validation through measured TDS and NO_3^{2-} by Schlumberger Water Services (2013)

The TDS anomalies (Fig. 13a) differ geographically concerning the concentration of NO_3^{2-} (Fig. 13b); it indicates two contamination sources contributed to dumping.

The first is the agricultural runoff (anthropogenic), and the other is the dissolution of rocks (lithogenic). NO_3^{2-} levels in the aquifer ranged between 1.7 and 338 mg/L (Fig. 13b). The high concentrations of NO_3^{2-} are mainly found in Wadis Baysh, Itwad, and Tabab. It is

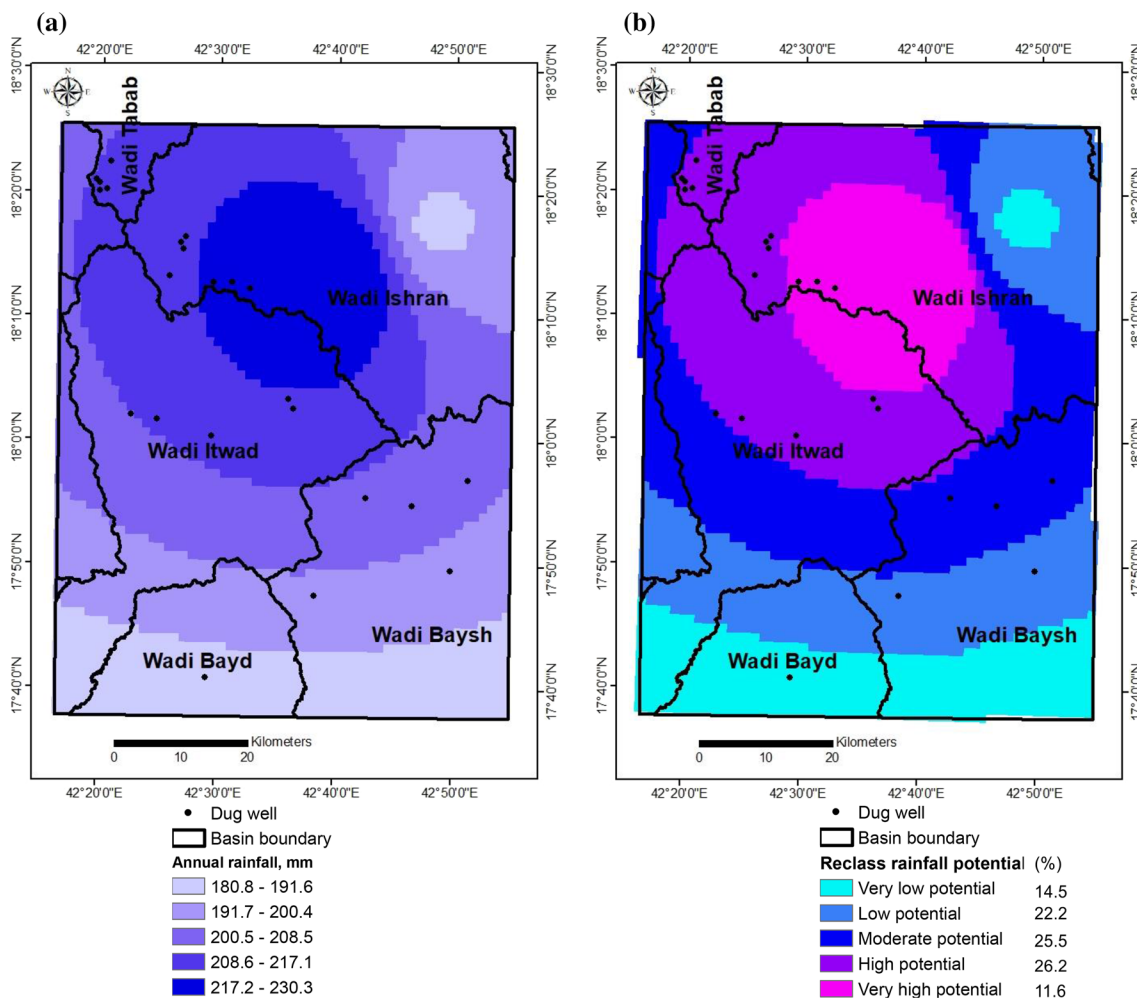


Fig. 11 a Average annual rainfall and b Reclassified rainfall of the study area

due to the intensive irrigated agriculture and the excessive and frequent use of mineral and organic fertilizer, which often exceeds the recommended limit (Zarhloule et al. 2009). In terms of land use, groundwater pollution by NO_3^{2-} is associated with vegetable cultivation (Fekkoul et al. 2013). The scattered samples have a NO_3^{2-} content of less than 10 mg/L, which shows no pollution and little use of fertilizers (Fig. 13b). The NO_3^{2-} content between 10 and 50 mg/L indicates moderate use of agricultural fertilizers, while above 50 mg/L reflects greater use of fertilizers (Fig. 13b). The higher concentration of the NO_3^{2-} and TDS concentrations reflected a low to very low potential due to poor aquifer quality. In comparison, the lower concentration indicates high to very high aquifer potentiality. In most areas, the aquifer was suitable for drinking and

irrigation purposes concerning TDS and NO_3^{2-} concentrations (Fig. 13a, b).

The TDS concentration increases in the northwestern part, matching with the greater area of low to very low aquifer potential (Figs. 12, 13a). The NO_3^{2-} content in groundwater increases in the southeastern part, which coincides with the greater area of low to very low aquifer potential (Figs. 12, 13b). The lowest TDS and NO_3^{2-} concentration in the aquifer (central and eastern part) matches the moderate to very high potential, confirming the model's results. It encourages the pursuit of research in areas with good potential for aquifers.

Validation through measured TDS in aquifer by Mallick et al. (2018)

The drilled dug wells number 3 and number 5 to 10 were located in moderate to very high potential zones (Fig. 14). The results of the model match with the dug sites data,

Fig. 12 Groundwater potential zones (GWPZs) map of the study area

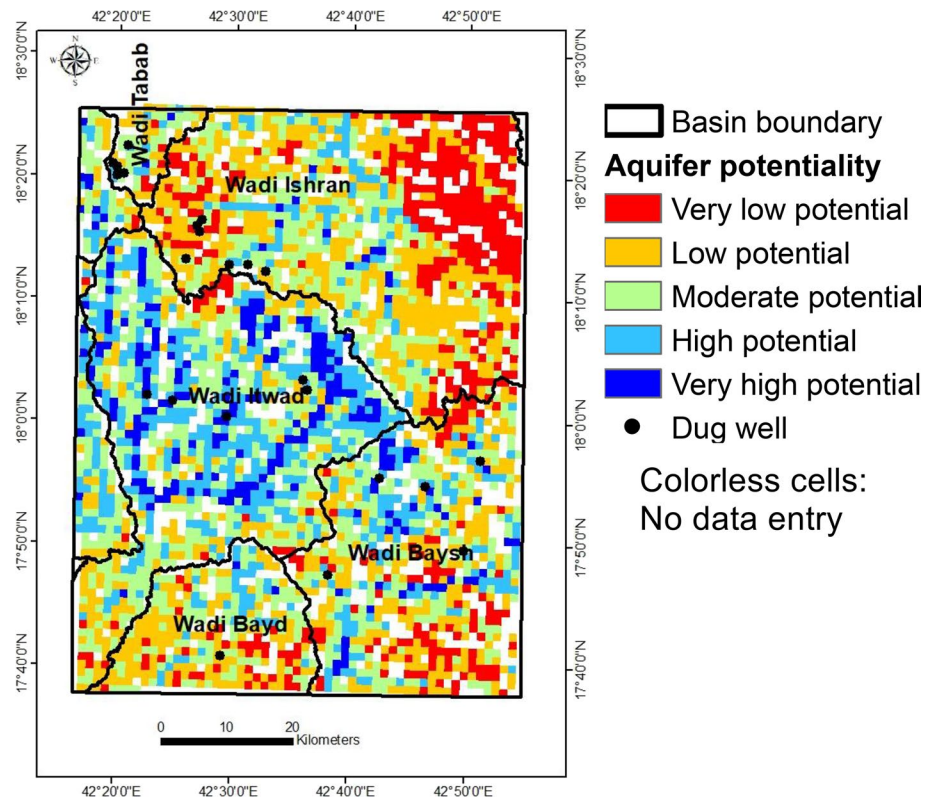


Table 3 Percent of the groundwater potential zones

| Zones | Weight class | Area (km ²) | Area (%) |
|---------------------|--------------|-------------------------|----------|
| Very low potential | 1 | 677.6 | 12.9 |
| Low potential | 2 | 1569.0 | 30.0 |
| Moderate potential | 3 | 1732.3 | 33.1 |
| High potential | 4 | 950.7 | 18.2 |
| Very high potential | 5 | 307.7 | 5.9 |

which shows a good sign for conducting the investigation in and around these dug sites to escalate the agricultural activity. It was observed that the concentration of TDS decreases in zone A (< 714 ppm) and increases in zone C (1028–1473 ppm). The northeastern part has the lowest TDS concentration and is characterized by very low potential. Consequently, the hydrogeochemical behaviors of the aquifer did not correspond to the model output. While in most of the remaining zones, the hydrogeochemical characteristics of the groundwater coincide with the model outputs. The previous results concluded that the most promising zones were in the western region with the lowest TDS concentration and a very high potential (Fig. 14).

Geophysical validation

The best promising area (Fig. 14) was characterized by a basement depth of < 500 m (Fig. 15a). It is better than deeper depths as the former was shallow and more attractive for exploration. The volcanic flow occurs at the surface and in the subsurface, surrounding (capped) the area to form a productive aquifer (Fig. 15b). The area (Fig. 14) was distinguished by a low magnetic anomaly (Fig. 15c) and a structural basin filled with Sabia Formation (Elawadi et al. 2012). The faults and grabens represent the main permeability, which receives leakage from rainfall or adjacent aquifers (Fig. 15c). The area was good for groundwater capping and therefore required further hydrogeological and hydrological investigation (Fig. 14).

Conclusion and recommendations

Several spatial studies were determined in the ArcGIS model to address the spatial challenges for aquifer recharge zones. The best prospective sites for aquifer potential were identified using GIS and RS approaches. These methods appear to be promising for defining GWPZs in the Aseer region. The aquifer potential zones are assessed using a

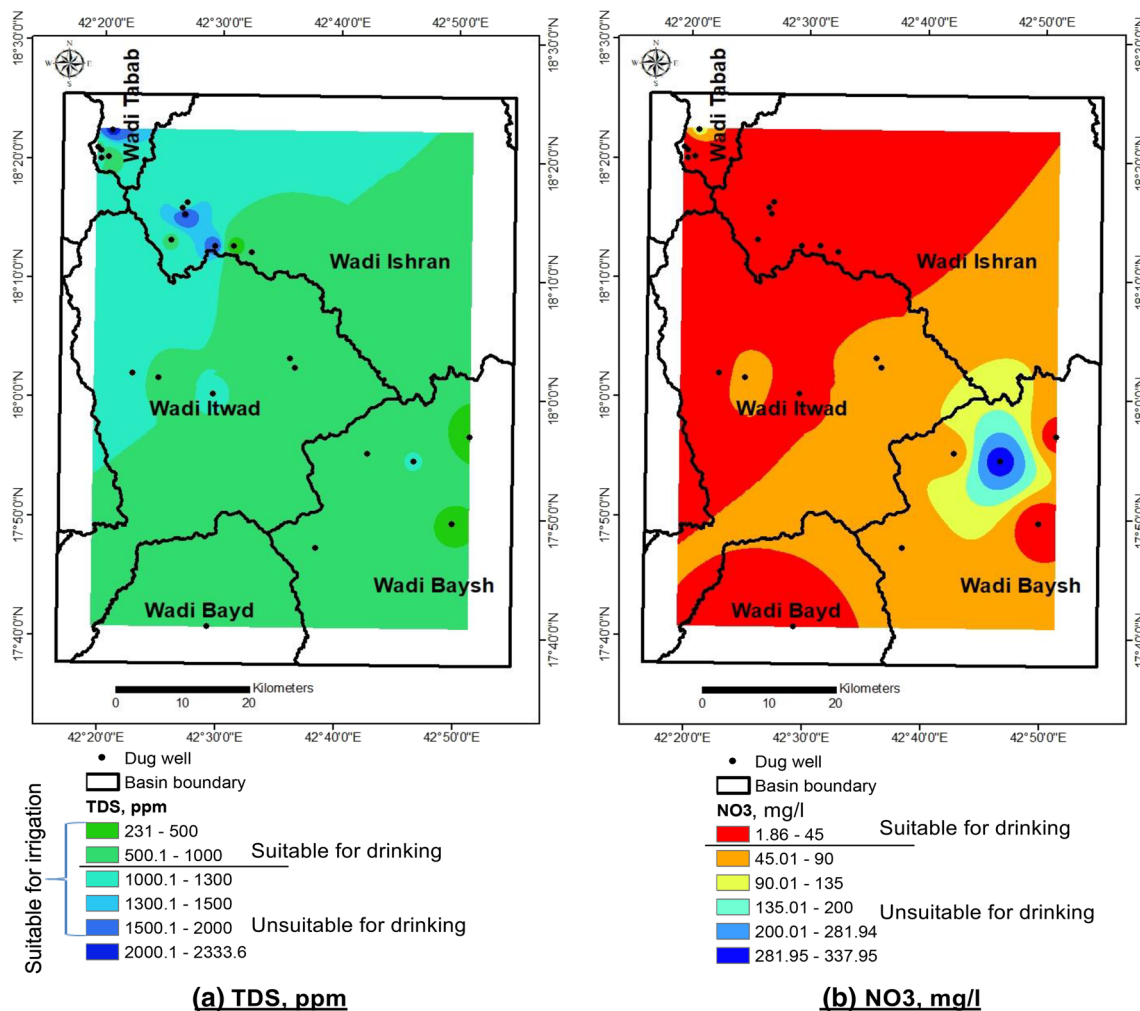


Fig. 13 a TDS and b NO_3^{2-} of the aquifer in the study area

weighted overlay analysis using spatial analyst tools. The latter has been found to be effective in terms of aquifer management in terms of time savings, low costs, planning, sustainability, and swift decision-making. Satellite images (L8SR), auxiliary data, and DEM were used to create all thematic maps, including lineaments, stream network, geology, slope, and NDVI. Thematic layers were created. Weights were applied to the thematic layers, which were then combined in a GIS model using weighted overlay analysis to produce the GWPZs map.

The current study revealed five categories of GWPZs: very low, low, moderate, high, and very high. Wadis, which is characterized by the presence of porosity and permeability, a gradual slope, and vegetation cover, has very

high to very high GWPZs. Approximately 6% to 18% of the land is classified as having very high and high potential aquifer recharge areas (suitable zones), while 33% is moderately appropriate and 43% has low and extremely low aquifer potential (unsuitable zones). The spatial distribution of high to very high GWPZs matches with dug well location, confirming the capabilities of RS and GIS for groundwater exploration and investment. Water quality and geophysical exploration were found to be very important indicators for delineating GWPZs. Based on the result of this study, the decision makers can find many unexplored areas of good aquifer potentiality.

Fig. 14 Dug sites and TDS concentration in the study area (reported by Mallick et al. 2018)

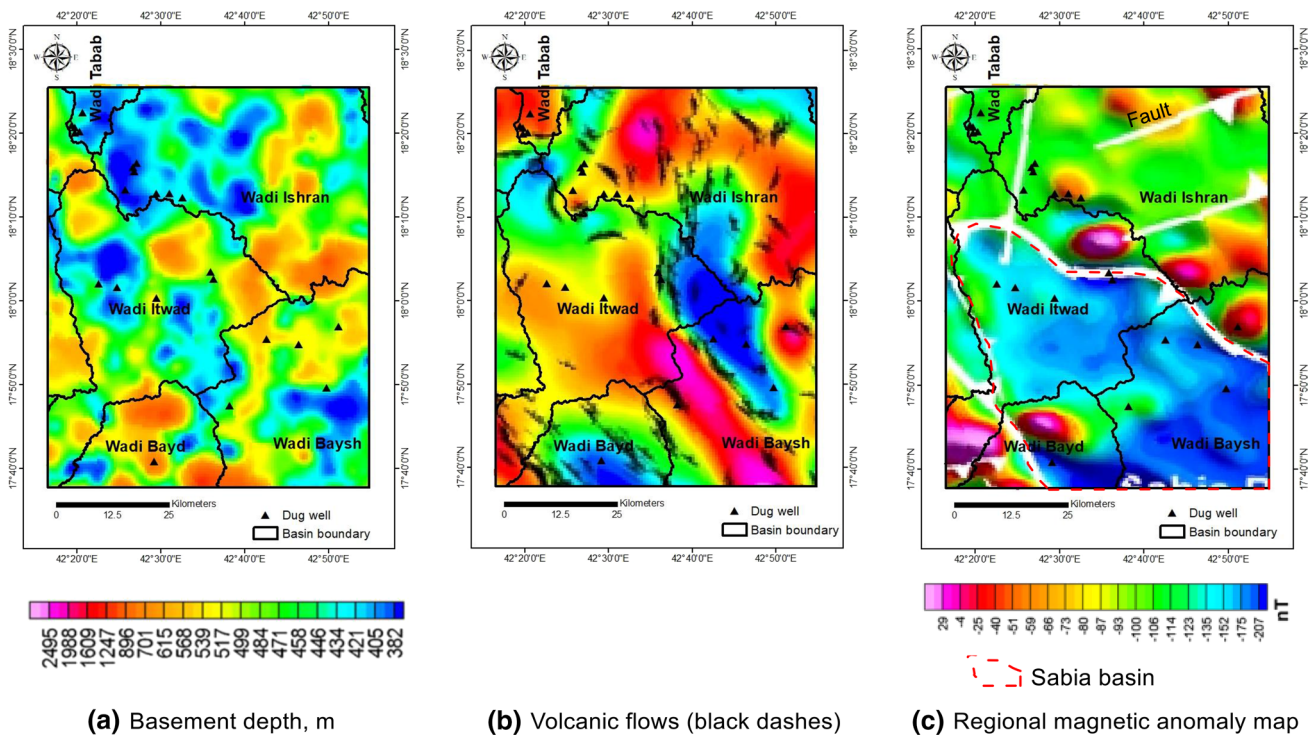
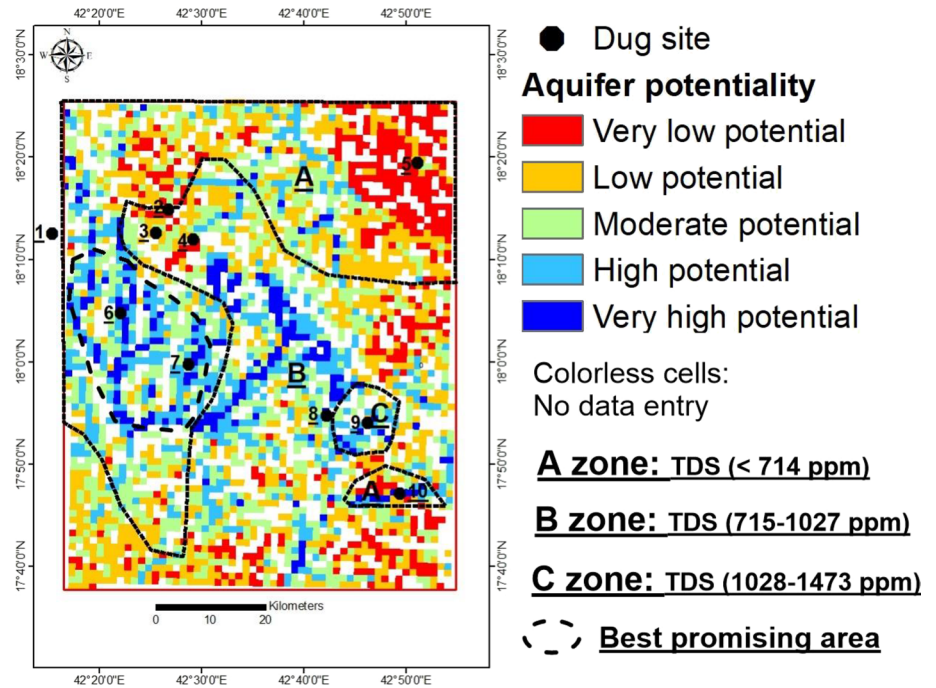


Fig. 15 a Magnetic sources, b source edge detection, and c regional anomaly magnetic map (after Elawadi et al. 2012)

Acknowledgements This research was funded by Institutional Funds Projects under Grant No. (IFPRC-098-145-2020). Therefore, authors gratefully acknowledge technical and financial support from Ministry of Education, Saudi Arabia and King Abdulaziz University, Jeddah, Saudi Arabia.

Funding This research was funded by Institutional Funds Projects under Grant No. (IFPRC-098-145-2020). Therefore, authors gratefully acknowledge technical and financial support from Ministry of Education and King Abdulaziz University, Jeddah, Saudi Arabia.

Declarations

Conflict of interest On behalf of all authors, the corresponding author states that there is no conflict of interest.

Human and animal rights This article does not contain any studies with human participants or animals performed by any of the authors.

Open Access This article is licensed under a Creative Commons Attribution 4.0 International License, which permits use, sharing, adaptation, distribution and reproduction in any medium or format, as long as you give appropriate credit to the original author(s) and the source, provide a link to the Creative Commons licence, and indicate if changes were made. The images or other third party material in this article are included in the article's Creative Commons licence, unless indicated otherwise in a credit line to the material. If material is not included in the article's Creative Commons licence and your intended use is not permitted by statutory regulation or exceeds the permitted use, you will need to obtain permission directly from the copyright holder. To view a copy of this licence, visit <http://creativecommons.org/licenses/by/4.0/>.

References

- Agarwal R, Garg PK (2016) Remote sensing and GIS based groundwater potential & recharge zones mapping using multi-criteria decision making technique. *Water Resour Manage* 30(1):243–260
- Algaydi BA, Subyani AM, Hamza MH (2019) Investigation of groundwater potential zones in hard rock terrain, Wadi Na'man. *Saudi Arab Groundw* 57(6):940–950
- Al-Ibrahim AA (1991) Excessive use of groundwater resources in Saudi Arabia: impacts and policy options. *Ambio* 34–37
- Al-Ruzouq R et al (2019) Potential groundwater zone mapping based on geo-hydrological considerations and multi-criteria spatial analysis: North UAE. *CATENA* 173:511–524
- Antonakos AK, Voudouris KS, Lambrakis NI (2014) Site selection for drinking-water pumping boreholes using a fuzzy spatial decision support system in the Korinthia prefecture, SE Greece. *Hydrogeol J* 22(8):1763–1776
- Arulbalaji P, Padmalal D, Sreelash K (2019) GIS and AHP techniques based delineation of groundwater potential zones: a case study from southern Western Ghats, India. *Sci Rep* 9(1):2082
- Balamurugan G, Seshan K, Bera S (2017) Frequency ratio model for groundwater potential mapping and its sustainable management in cold desert, India. *J King Saud Univ Sci* 29(3):333–347
- Barik KK, Dalai PC, Goudo SP, Panda SR, Nandi D (2017) Delineation of groundwater potential zone in Baliguda Block of Kandhamal District, Odisha using geospatial technology approach. *Int J Adv Remote Sens GIS* 6(3):2068–2079
- Blank R, Johnson P, Gettings M, Simmons G (1985) Explanatory notes to the geologic map of the Jizan quadrangle (Jiddah, Saudi Arabia: Deputy Minister for Mineral Resources, p 24
- Brito TP et al (2020) Assessment of the groundwater favorability of fractured aquifers from the southeastern Brazil crystalline basement. *Hydrol Sci J* 65(3):442–454
- Chen W et al (2018) GIS-based groundwater potential analysis using novel ensemble weights-of-evidence with logistic regression and functional tree models. *Sci Total Environ* 634:853–867
- Chowdhury A, Jha MK, Chowdary VM (2010) Delineation of groundwater recharge zones and identification of artificial recharge sites in West Medinipur district, West Bengal, using RS, GIS and MCDM techniques. *Environ Earth Sci* 59(6):1209
- Corsini A, Cervi F, Ronchetti F (2009) Weight of evidence and artificial neural networks for potential groundwater spring mapping: an application to the Mt. Modino area (Northern Apennines, Italy). *Geomorphology* 111:79–87
- Das B, Pal SC (2019) Assessment of groundwater recharge and its potential zone identification in groundwater-stressed Goghat-I block of Hugli District, West Bengal, India. *Environ Dev Sustain* 1–19
- Deepa S, Venkateswaran S, Ayyandurai R, Kannan R, Prabhu MV (2016) Groundwater recharge potential zones mapping in upper Manimuktha Sub basin Vellar river Tamil Nadu India using GIS and remote sensing techniques. *Model Earth Syst Environ* 2(3):1–13
- Eastman JR, Jin W, Kyem P, Toledano J (1995) Raster procedure for multicriterial multi-objective decisions. *Photogramm Eng Remote Sens* 61:539–547
- Edet AE, Okereke CS, Teme SC, Esu EO (1998) Application of remote sensing data to groundwater exploration: a case study of the Cross River State, southeastern Nigeria. *J Hydrogeol* 6:394–404
- Elawadi E, Mogren S, Ibrahim E, Batayneh A, Al-Bassam A (2012) Utilizing potential field data to support delineation of groundwater aquifers in the southern Red Sea coast, Saudi Arabia. *J Geophys Eng* 9(3):327–335
- Elewa HH, Qaddah AA (2011) Groundwater potentiality mapping in the Sinai Peninsula, Egypt, using remote sensing and GIS-watershed-based modeling. *Hydrogeol J* 19(3):613–628
- Fekkoul A, Zarhloule Y, Boughriba M, Barkaoui AE, Jilali A, Bouri S (2013) Impact of anthropogenic activities on the groundwater resources of the unconfined aquifer of Triffa plain (Eastern Morocco). *Arab J Geosci* 6(12):4917–4924
- Fildes SG, Clark IF, Somaratne NM, Ashman G (2020) Mapping groundwater potential zones using remote sensing and geographical information systems in a fractured rock setting, Southern Flinders Ranges, South Australia. *J Earth Syst Sci* 129(1):1–25
- Fitts CR (2002) *Groundwater science*. Elsevier, London, UK
- Golkarian A et al (2018) Groundwater potential mapping using C5.0, random forest, and multivariate adaptive regression spline models in GIS. *Environ Monit Assessment* 190:149
- Gupta M, Srivastava PK (2010) Integrating GIS and remote sensing for identification of groundwater potential zones in the hilly terrain of Pavagarh, Gujarat, India. *Water Int* 35(2):233–245
- Gyeltshen S, Tran TV, Teja Gunda GK, Kannaujya S, Chatterjee RS, Champatiray PK (2020) Groundwater potential zones using a combination of geospatial technology and geophysical approach: case study in Dehradun, India. *Hydrol Sci J* 65(2):169–182
- Hussein MT, Ibrahim KE (1997) Electrical resistivity, geochemical and hydrogeological properties of wadi deposits, Western Saudi Arabia. *Earth Sci* 9(1):55–72
- Israil M, Al-hadithi M, Singhal DC (2006) Application of a resistivity survey and geographical information system (GIS) analysis for

- hydrogeological zoning of a piedmont area, Himalayan foothill region, India. *Hydrogeol J* 14(5):753–759
- Jaiswal RK, Mukherjee S, Krishnamurthy J, Saxena R (2003) Role of remote sensing and GIS techniques for generation of groundwater prospect zones towards rural development—an approach. *Int J Remote Sens* 24(5):993–1008
- Jha MK, Chowdary VM, Chowdhury A (2010) Groundwater assessment in Salboni Block, West Bengal (India) using remote sensing, geographical information system and multi-criteria decision analysis techniques. *Hydrogeol J* 18(7):1713–1728
- Kamali Maskooni E et al (2020) Application of advanced machine learning algorithms to assess groundwater potential using remote sensing-derived data. *Remote Sens* 12(17):2742
- Kamruzzaman MM, Alanazi SA, Alruwaili M, Alshammari N, Siddiqi MH, EnamulHuq MD (2020). Water resource evaluation and identifying groundwater potential zones in Arid area using remote sensing and geographic information system. *J Comput Sci* 2020, 16 (3): 266.279.
- Khan MYA, Wen J (2021) Evaluation of physicochemical and heavy metals characteristics in surface water under anthropogenic activities using multivariate statistical methods, Garra River, Ganges Basin, India. *Environ Eng Res*. <https://doi.org/10.4491/eer.2020.280>
- Khan MYA, ElKashouty M, Bob M (2020) Impact of rapid urbanization and tourism on the groundwater quality in Al Madinah city, Saudi Arabia: a monitoring and modeling approach. *Arab J Geosci* 13(18):1–22
- Krishnamurthy J, Venkatesesa KN (1996) An approach to demarcate ground water potential maps through remote sensing and GIS. *Int J Remote Sens* 7:1867–1884
- Kumar SS (1987) National remote sensing agency. In: Proceedings of the international conference on groundwater systems under stress: Brisbane, Australia, 11 to 16 May 1986 (No. 13). Australian Government Publishing Service, p 375
- Kumar A, Sharma MP, Yadav NS (2014) Assessment of water quality changes at two locations of Chambal River: MP. *J Mater Environ Sci* 5(6):1781–1785
- Kumar A, Sharma MP, Taxak AK (2017) Analysis of water environment changing trend in Bhagirathi tributary of Ganges in India. *Desalin Water Treat* 63:55–62
- Kumar A, Taxak AK, Mishra S, Pandey R (2021) Long term trend analysis and suitability of water quality of River Ganga at Himalayan hills of Uttarakhand, India. *Environ Technol Innov* 22:101405
- Lee S et al (2012) Regional groundwater productivity potential mapping using a geographic information system (GIS) based artificial neural network model. *Hydrogeol J* 20(8):1511–1527
- Li Y, Khan MYA, Jiang Y, Tian F, Liao W, Fu S, He C (2019) CART and PSO+ KNN algorithms to estimate the impact of water level change on water quality in Poyang Lake, China. *Arab J Geosci* 12(9):1–12
- Machiwal D, Jha MK, Mal BC (2011) Assessment of groundwater potential in a semi-arid region of India using remote sensing, GIS and MCDM techniques. *Water Resour Manage* 25(5):1359–1386
- Mallick J, Singh CK, AlMesfer MK, Kumar A, Abad Khan R, Islam S, Rahman A (2018) Hydro-geochemical assessment of groundwater quality in Aseer Region, Saudi Arabia. *Water* 2018(10):1847
- Manap MA et al (2014) Application of probabilistic-based frequency ratio model in groundwater potential mapping using remote sensing data and GIS. *Arab J Geosci* 7(2):711–724
- Mishra S, Kumar A, Shukla P (2021) Estimation of heavy metal contamination in the Hindon River, India: an environmental approach. *Appl Water Sci* 11(1):1–9
- Moghaddam DD et al (2015) Groundwater spring potential mapping using bivariate statistical model and GIS in the Taleghan watershed, Iran. *Arab J Geosci* 8(2):913–929
- Mogren S, Batayneh A, Elawadi E, Al-Bassam A, Ibrahim E, Qaisy S (2011) Aquifer boundaries explored by geoelectrical measurements in the Red Sea coastal plain of Jazan area, South west Saudi Arabia. *Int J Phys Sci* 6:3768–76
- Mukherjee I, Singh UK (2020) Delineation of groundwater potential zones in a drought-prone semi-arid region of east India using GIS and analytical hierarchical process techniques. *CATENA* 194:104681
- Mukherjee P, Singh CK, Mukherjee S (2012) Delineation of groundwater potential zones in arid region of India—a remote sensing and GIS approach. *Water Resour Manage* 26(9):2643–2672
- Mumtaz R et al (2019) Delineation of groundwater prospective resources by exploiting geospatial decision-making techniques for the Kingdom of Saudi Arabia. *Neural Comput Appl* 31(9):5379–5399
- MWE (2012) Supporting documents for King Hassan II Great Water prize. http://www.worldwatercouncil.org/fileadmin/www/Prizes/Hassan_II/Candidates_2011/16.Ministry_
- Naghibi SA, Pourghasemi HR (2015) A comparative assessment between three machine learning models and their performance comparison by bivariate and multivariate statistical methods in groundwater potential mapping. *Water Resour Manage* 29(14):5217–5236
- Nampak H, Pradhan B, Manap MA (2014) Application of GIS based data driven evidential belief function model to predict groundwater potential zonation. *J Hydrol* 513:283–300
- Oh HJ et al (2011) GIS mapping of regional probabilistic groundwater potential in the area of Pohang City, Korea. *J Hydrol* 399(3–4):158–172
- Ouda O (2014) Water demand versus supply in Saudi Arabia: current and future challenges. *Int J Water Resour Dev* 30(2):335–344
- Ozdemir A (2011) GIS-based groundwater spring potential mapping in the Sultan Mountains (Konya, Turkey) using frequency ratio, weights of evidence and logistic regression methods and their comparison. *J Hydrol* 411(3–4):290–308
- Prasad P et al (2020) Application of machine learning techniques in groundwater potential mapping along the west coast of India. *Gisci Remote Sens* 57(6):735–752
- Rao Y, Jugran DK (2003) Delineation of groundwater potential zones and zones of groundwater quality suitable for domestic purposes using remote sensing and GIS. *HydroSci* 48(5):821–833
- Rodell M, Velicogna I, Famiglietti JS (2009) Satellite-based estimates of groundwater depletion in India. *Nature* 460(7258):999
- Salama RB (1997) Geomorphology, geology and palaeohydrology of the broad alluvial valleys of the Salt River System, Western Australia. *Aust J Earth Sci* 44(6):751–765
- Sandoval JA, Tiburan CL Jr (2019) Identification of potential artificial groundwater recharge sites in Mount Makiling Forest Reserve, Philippines using GIS and Analytical Hierarchy Process. *Appl Geogr* 105:73–85
- Schlumberger Water Services (2013) Assir directorate final report. Ministry of water and electricity, Kingdom wide-drinking water quality study
- Sener E, Davraz A, Ozcelik M (2005) An integration of GIS and remote sensing in groundwater investigations: a case study in Burdur, Turkey. *Hydrogeol J* 13:826–834
- Singh LK, Jha MK, Chowdary VM (2018) Assessing the accuracy of GIS-based Multi-Criteria Decision Analysis approaches for mapping groundwater potential. *Ecol Ind* 91:24–37
- Singhal BBS, Gupta RP (1999) Remote sensing. In: Applied hydrogeology of fractured rocks (pp 53–86). Springer, Dordrecht
- Souissi D et al (2018) Mapping groundwater recharge potential zones in arid region using GIS and Landsat approaches, southeast Tunisia. *Hydro Sci J* 63(2):251–268
- Sreedhar G, Vijaya Kumar GT, Murali Krishna IV, Ercan K, Cüneyd DM (2009) Mapping of groundwater potential zones in the

- Musi basin using remote sensing data and GIS. *Adv Eng Softw* 40:506–518
- Tahmassebi N et al (2016) Spatial analysis of groundwater potential using weights-of-evidence and evidential belief function models and remote sensing. *Arab J Geosci* 9(1):79
- Teeuw RM (1995) Groundwater exploration using remote sensing and a low-cost geographical information system. *Hydrogeol J* 3(3):21–30
- Teeuw RM (1999) Groundwater exploration using remote sensing and a low cost GIS. *J Hydrogeol* 3:21–30
- Vincent P (2008) Saudi Arabia: an environmental overview. Taylor and Francis, London. <https://doi.org/10.1201/9780203030882>
- Voogd H (1983) Multi-criteria evaluation for urban and regional planning. Pion, London. *Water Resour Manag* 24(5):921–939
- Wieland M, Pittore M (2017) A spatio-temporal building exposure database and information life-cycle management solution. *ISPRS Int J Geo Inf* 6(4):114
- World Bank (2005) A water sector assessment report on countries of the cooperation council of the Arab State of the Gulf. (Report No. 32539-MNA). Washington, USA
- Zarhloule Y, Fekkoul F, Boughriba M, Kabbabi A, Carneiro J, Correia A, Rimi A, Houadi B (2009) Climate change and human activities Impact on the groundwater of the Eastern Morocco: case of Triffa Plain and shallow coastal Mediterranean aquifer at Saïdia. *Innovation in groundwater governance in MENA region*. *JSIW* 13:14–17

Publisher's Note Springer Nature remains neutral with regard to jurisdictional claims in published maps and institutional affiliations.